Hindawi
Advances in Tribology
Volume 2018, Article ID 3981087, 7 pages
https://doi.org/10.1155/2018/3981087

Research Article

A Study of Hydromagnetic Longitudinal Rough Circular Step Bearing

Jatinkumar V. Adeshara,[1] M. B. Prajapati,[2] G. M. Deheri,[3] and R. M. Patel[4]

[1]*Research Scholar, Department of Mathematics, H. N. G. University, Patan, 384 265, Gujarat State, India*
[2]*Head, Department of Mathematics, HNG University, Patan 384 265, Gujarat, India*
[3]*Department of Mathematics, SP University, Vallabh Vidyanagar 388 120, Gujarat, India*
[4]*Department of Mathematics, Gujarat Arts and Science College, Ahmedabad 380 006 Gujarat, India*

Correspondence should be addressed to R. M. Patel; rmpatel2711@gmail.com

Received 13 May 2018; Accepted 10 July 2018; Published 2 September 2018

Academic Editor: Huseyin Çimenoğlu

This article discusses the effect of longitudinal roughness on the performance of hydromagnetic squeeze film in circular step bearing. To characterize the random roughness of the bearing surfaces the stochastic model of Christensen and Tonder has been employed. The stochastically averaged Reynolds' type equation is solved using suitable boundary conditions to obtain the pressure distribution and then the load bearing capacity is computed. The results are presented in graphical form. The graphical results presented here establish that the hydromagnetic lubrication offers significant help to the longitudinal roughness pattern to enhance the performance of the bearing system. Of course, conductivities of the plates, standard deviation, and the supply pressure contribute towards reducing the negative effect induced by variance (+ve) and skewness (+ve).

1. Introduction

It is documented that gears, braking units, hydraulic dampers, skeletal bearings, and synovial joints make use of squeeze film mechanism. Generally an electrically conducting fluid with high thermal and electrical conductivity is applied as a lubricant for squeeze film to work under such extreme circumstances. Also, a use of external magnetic field then advances the performance of lubrication.

The performance of an oil lubricated circular step bearing is analyzed by Majumdar [1]; this study underlines the importance of radii ratio. Lin [2] discussed the couple stress effect on the performance of an externally pressurized circular step bearing. It was established that the couple stress fluid modified the performance of the bearing system. Deheri et al. [3] reformed and developed the study of Majumdar [1] to use the magnetization effect by considering a magnetic fluid as the lubricant, the flow being regulated by Neuringer–Rosensweig's model [4].

It is well known that the effect of surface roughness is quite important in different types of bearing systems. Most of the discussions have considered the stochastic averaging method of Christensen and Tonder [5–7] who presented a stochastic model to evaluate the effect of rough surfaces. (Ting [8], Prakash and Tiwari [9], Prajapati [10], and Andharia et al. [11]).

The hydromagnetic squeeze films between two conducting rough circular plates are studied by Vadher et al. [12]. It was investigated that the negative effect of roughness got minimized up to some extent by applying magnetization. Patel and Deheri [13] evaluated the performance of ferrofluid squeeze film in rotating curved circular plates by using Shliomis model. Here, the outcomes of this article suggested that Shliomis model based ferrofluid lubrication was relatively better than the model of Neuringer–Rosensweig [4]. Patel et al. [14] extended the study of Deheri et al. [3] to study the effect of transverse surface roughness. It was indicated that the bearing performance was adversely affected by the roughness of the bearing surfaces. But the situation was found to be a little enhanced in case of variance (-ve) was considered. A modified lubrication equation for hydromagnetic

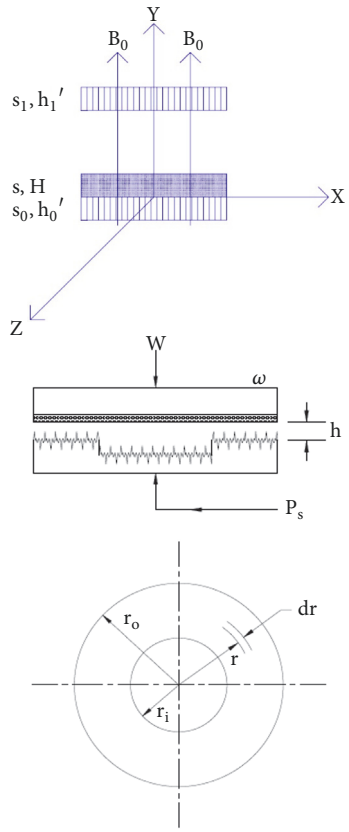

Figure 1: Configuration of bearing system.

non-Newtonian cylindrical squeeze films was presented by Lin et al. [15]. The hydromagnetic non-Newtonian effects offered quite better performance for circular squeeze films in comparison with the case of a nonconducting Newtonian lubricant.

Patel and Deheri [16] studied the magnetic fluid lubrication of a squeeze film in transversely rough porous circular plates with concentric circular pocket. Longitudinal roughness effect has been a matter of discussions in Andharia and Deheri [17], Andharia and Deheri [18], Andharia and Deheri [19], and Shimpi and Deheri [20]. Recently, Lin [21] examined the ferrofluid lubrication of a longitudinally rough journal bearing.

Patel et al. [22] discussed the hydromagnetic lubrication of a rough porous circular step bearing. Hence, it has been sought to analyze the effect of longitudinal roughness pattern on behavior of a hydromagnetic squeeze film in circular step bearings.

2. Analysis

The configuration of the bearing system is presented in Figure 1.

For the computation of different performance characteristics, generally the following assumptions are considered:

(1) The recess is deep enough for the pressure in it to be uniform.

(2) The bearing has very low rotational velocity and its effect is neglected for the pressure generation.

As shown in Figure 1 a thrust load w is applied and the bearing supports the load without metal to metal contact. The load w is supported by the fluid within the pocket and land. The fluid escapes in the radial direction through the restrictions by a land or sill around the recess.

In view of the discussions of Christensen and Tonder [5–7] the surfaces of bearing are taken to be longitudinally rough. The thickness h(x) of the lubricant film is given by

$$h(x) = \overline{h}(x) + h_s \tag{1}$$

where $\overline{h}(x)$ is the mean film thickness and h_s is the deviation from the mean film thickness characterizing the random roughness surface. h_s is considered in nature and governed by the probability density function $f(h_s)$, $-c \le f(h_s) \le c$, where c is the maximum deviation from the mean film thickness. The mean α and standard deviation σ and the measure of symmetry ε of the random variable h_s are defined by the relationships.

$$\begin{aligned} \alpha &= E(h_s) \\ \sigma^2 &= E\left[(h_s - \alpha)^2\right] \end{aligned} \tag{2}$$

and

$$\varepsilon = E\left[(h_s - \alpha)^3\right] \tag{3}$$

where E denotes the expected value defined by

$$E(R) = \int_{-c}^{c} Rf(h_s)\, dh_s \tag{4}$$

The concerned Reynolds' type equation gives the pressure induced flow for a circular step bearing as (Majumdar (1985), Patel, Deheri, and Vadher (2015))

$$Q = -\frac{2\pi r (dp/dr)\left[\left(2/M^3 m(h)\right)[M/2 - \tanh(M/2)]\right]\left[\left(\phi_0 + \phi_1 + 1\right)/\left(\phi_0 + \phi_1 + (\tanh(M/2))/(M/2)\right)\right]}{12\mu} \tag{5}$$

where

$$m(h) = h^{-3}\left[1 - 3\alpha h^{-1} + 3h^{-2}\left(\sigma^2 + \alpha^2\right) - \frac{3}{40}h^{-3}\left(\varepsilon + 3\sigma^2\alpha + \alpha^3\right)\right] \tag{6}$$

Using Reynolds' boundary conditions

$$\begin{aligned} r &= r_o; \\ p &= 0; \end{aligned}$$

$$\begin{aligned} r &= r_i; \\ p &= p_s; \end{aligned} \tag{7}$$

the governing equation for the film pressure p is given by

$$p = p_s \frac{\ln(r/r_o)}{\ln(r_i/r_o)} \tag{8}$$

where in

$$p_s = \frac{6}{\pi\left[(2/M^3 m(h))[M/2 - \tanh(M/2)]\right]\left[\left(\phi_0 + \phi_1 + 1\right)/\left(\phi_0 + \phi_1 + (\tanh(M/2))/(M/2)\right)\right]} \ln\left(\frac{r_o}{r_i}\right) \tag{9}$$

Introduction of the dimensionless terms

$$\begin{aligned} P_s^* &= \frac{6\ln(1/k)}{\pi\left((2/M^3)/(M*(h))\right)[M/2 - \tanh(M/2)]\left[\left(\phi_0 + \phi_1 + 1\right)/\left(\phi_0 + \phi_1 + (\tanh(M/2))/(M/2)\right)\right]} \\ M*(h) &= m(h)\, h^3 = \left(1 - 3\alpha^* + 3\left(\alpha^{*2} + \sigma^{*2}\right) - \frac{3}{40}\left(\varepsilon^* + 3\sigma^{*2}\alpha^* + \alpha^{*3}\right)\right) \\ \alpha^* &= \left(\frac{\alpha}{h}\right) \\ \sigma^* &= \left(\frac{\sigma}{h}\right) \\ \varepsilon^* &= \left(\frac{\varepsilon}{h^3}\right) \\ k &= \left(\frac{r_i}{r_o}\right) \end{aligned} \tag{10}$$

paves the way for the expression of pressure distribution in nondimensional form as

$$P = P_s^* \frac{\ln(r/r_o)}{\ln(r_i/r_o)} \tag{11}$$

The load bearing capacity w is calculated by integrating the pressure which takes the dimensionless form

$$W = \frac{P_s^* \ln\left(1 - k^2\right)}{\ln(1/k)} \tag{12}$$

3. Results and Discussions

The representation for dimensionless pressure profile is given in (11) while the nondimensional load bearing capacity is governed by (12). From these equations it is clearly observed that the load carrying capacity

$$W \propto P_s^* \tag{13}$$

and

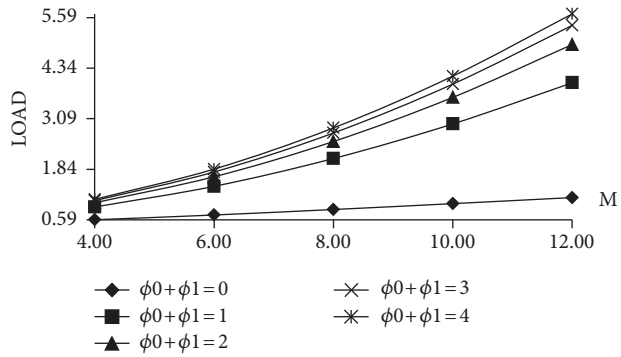

Figure 2: Variation of load carrying capacity with respect to M and $\phi_0 + \phi_1$.

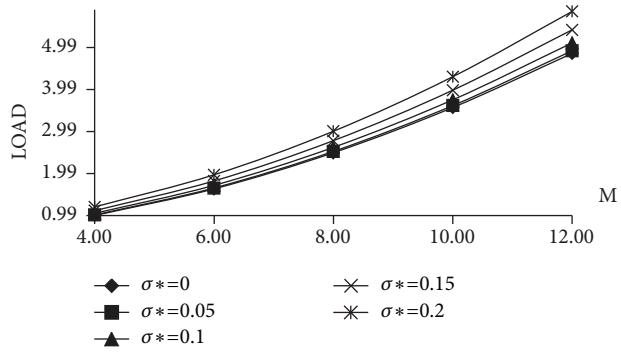

Figure 3: Distribution of load bearing capacity with respect to M and σ^*.

$$p_s = \frac{Q}{\left(\left(2/M^3\right)/m\,(h)\right)\left[M/2 - \tanh\left(M/2\right)\right]\left[\left(\phi_0 + \phi_1 + 1\right)/\left(\phi_0 + \phi_1 + \left(\tanh\left(M/2\right)\right)/\left(M/2\right)\right)\right]} \tag{14}$$

This suggests that for a constant flow rate the load increases as stochastically averaged squeeze film thickness decreases. Therefore, the bearing turns out to be self-compensating provided the flow rate is considered as constant. It is depicted from (11) and (12) that the effect of conductivity parameters on the distribution of pressure and load bearing capacity is determined by

$$\frac{\phi_0 + \phi_1 + \left(\tanh\left(M/2\right)\right)/\left(M/2\right)}{\phi_0 + \phi_1 + 1} \tag{15}$$

which turns to

$$\frac{\phi_0 + \phi_1}{\phi_0 + \phi_1 + 1} \tag{16}$$

for large values of M, because $\tanh(M) \cong 1$ and $(2/M) \cong 0$. Further, it is noticed that the pressure and load carrying capacity increases with increases in $\phi_0 + \phi_1$ because both the functions are increasing functions of $\phi_0 + \phi_1$.

It is clearly depicted from Figures 2–6 that the hydromagnetization parameter induces a sharp increase in the load bearing capacity while Figures 7–10 gives the profile of load with respect to $\phi_0 + \phi_1$ for different values of standard deviation, variance, skewness, and radii ratio, respectively. Here, also the load carrying capacity increases with an increase in conductivity parameter. Figures 7–10 also tells that the load increases sharply up to some extent ($\phi_0 + \phi_1 \cong 1.32$) and then this rate of increase gets slower.

It is seen from Figures 11–13 that the standard deviation associated with longitudinal roughness causes increased load bearing capacity with respect to various parameters such as variance, skewness, and radii ratio. Besides, variation of load carrying capacity for different values of variance is described by Figures 14 and 15. From these figures it is noticed that the load decreases with increase in positive variance while the variance (− ve) increases it. The trends of load bearing capacity with respect to skewness are similar to that of variance which is observed from Figure 16.

Form Figures 5 and 9 it is clearly observed that the effect of ε^* on the variation of load carrying capacity with respect to magnetization and conductivity, respectively, remains negligible while this effect of ε^* with regards to variance is registered to be nominal as suggested by Figure 14.

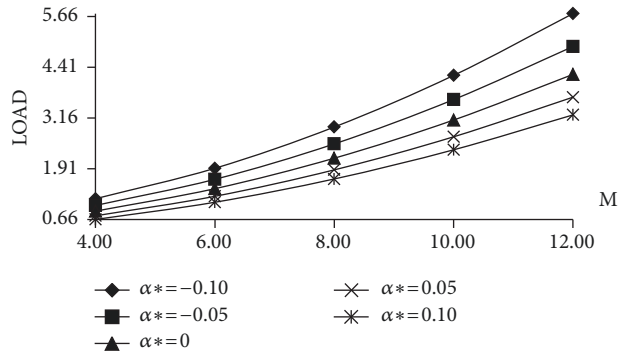

Figure 4: Profile of load with respect to M and α^*.

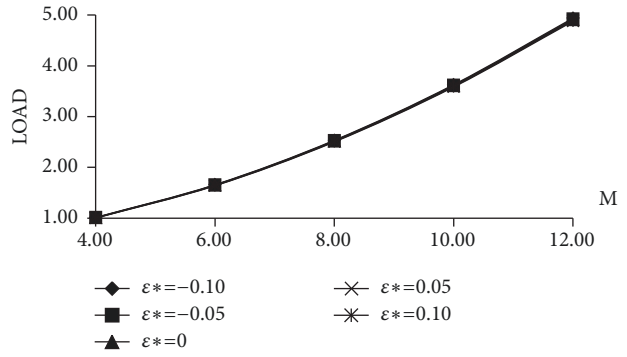

Figure 5: Variation of load carrying capacity with respect to M and ε^*.

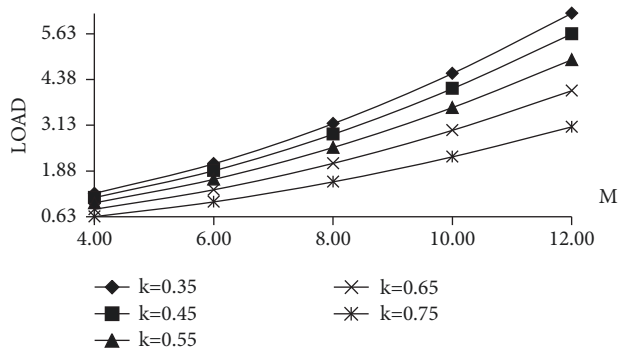

Figure 6: Distribution of load bearing capacity with respect to M and k.

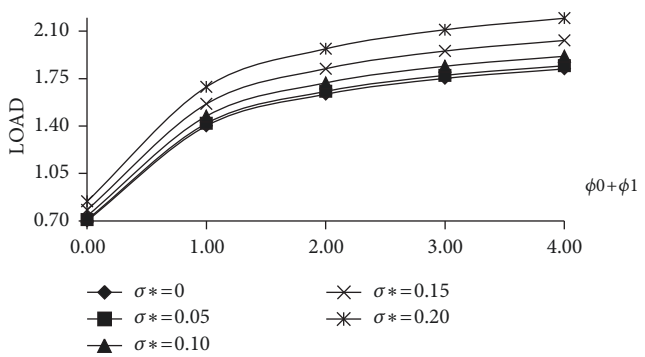

Figure 7: Profile of load with respect to $\phi_0 + \phi_1$ and σ^*.

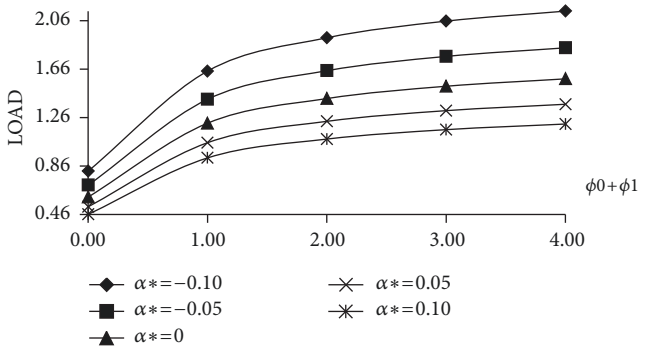

Figure 8: Variation of load carrying capacity with respect to $\phi_0 + \phi_1$ and α^*.

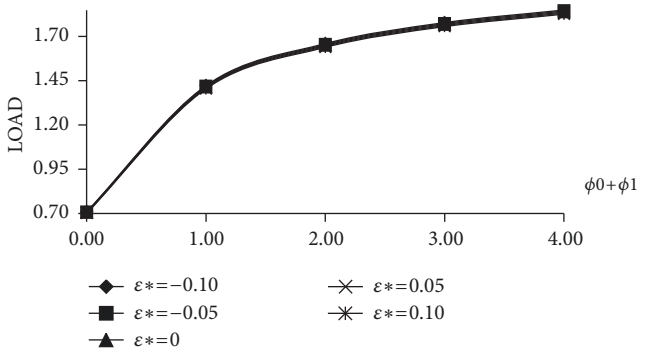

Figure 9: Distribution of load bearing capacity with respect to $\phi_0 + \phi_1$ and ε^*.

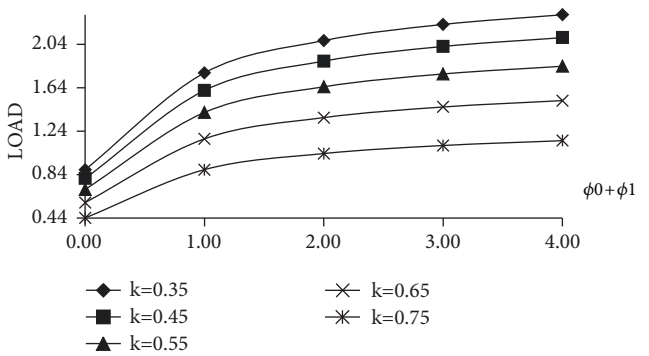

Figure 10: Profile of load with respect to $\phi_0 + \phi_1$ and k.

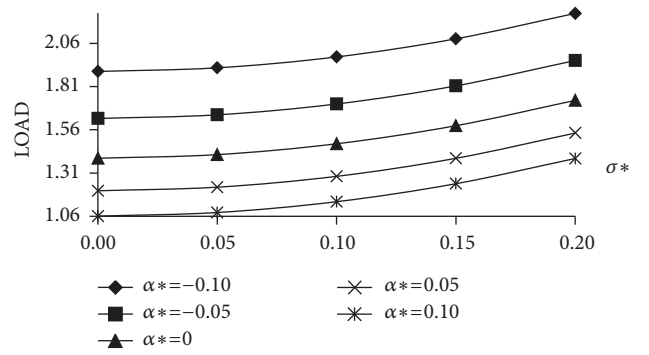

Figure 11: Variation of load carrying capacity with respect to σ^* and α^*.

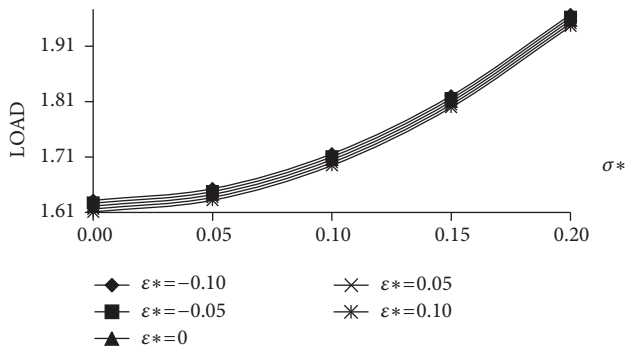

Figure 12: Distribution of load bearing capacity with respect to σ^* and ε^*.

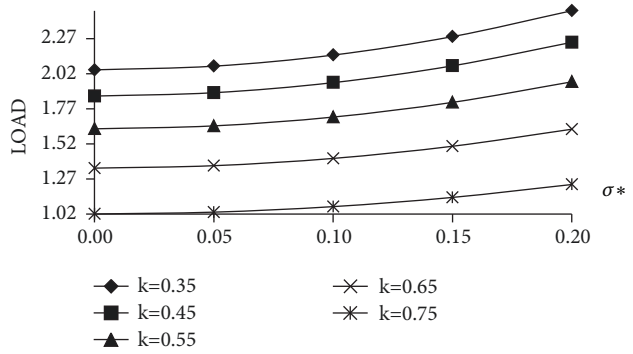

Figure 13: Profile of load with respect to σ^* and k.

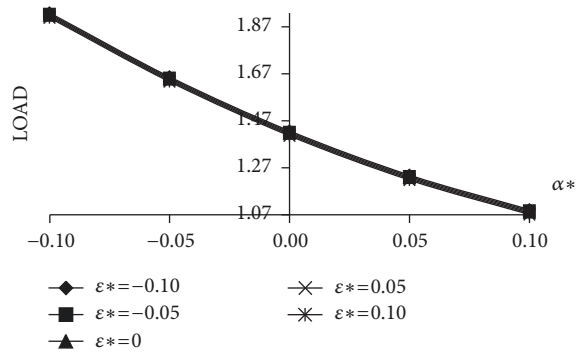

Figure 14: Variation of load carrying capacity with respect to α^* and ε^*.

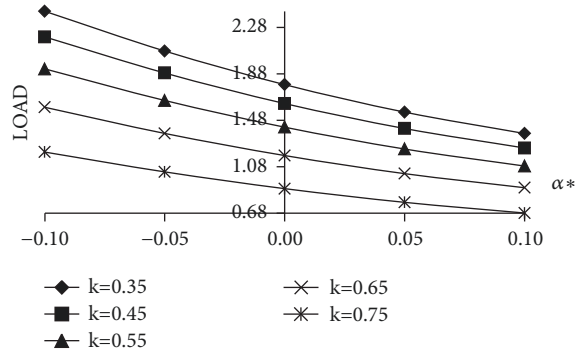

Figure 15: Distribution of load bearing capacity with respect to α^* and k.

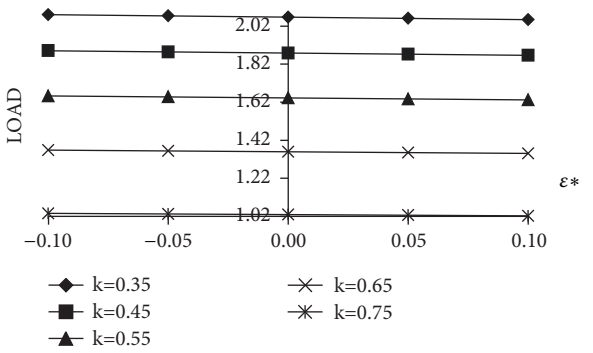

Figure 16: Profile of load with respect to ε^* and k.

This means that this type of bearing system the suitable combination of negatively skewed roughness and negative variance may go a long way for better performance of the bearing system.

It is seen that for small as well as large values of M the performance of the bearing suffers when the plates are considered to be electrically conducting, in matching with the hydromagnetic case, when the plates are taken to be nonconducting. Further, this can physically be clarified by fringing phenomena which happens when the plates are electrically conducting. Finally, the load is acquired to be more in comparison with the Neuringer Rosensweig model based ferrofluid squeeze film.

4. Conclusions

The trio of hydromagnetization, supply pressure, and standard deviation counters fruitfully the negative effect induced by positively skewed roughness and variance (+ve) in the case of negatively skewed roughness when variance comes out to be negative. Of course, in bettering the bearing performance the plate conductivities and radii ratio may play an important role. Needless to say, the longitudinal roughness parameter behaves in a little better way as compared to the transverse roughness. Therefore, it becomes very much essential that the longitudinal roughness aspect must be given due consideration from longevity point of view while designing this type of bearing system.

Nomenclature

r: Radial coordinate
r_o: Outer radius
r_i: Inner radius
k: Radii ratio (r_i/r_o)
h: Lubricant film thickness
H: Thickness of solid housing
s: Electrical conductivity of the lubricant
μ: Viscosity of the lubricant
B_o: Uniform transverse magnetic field applied between the plates
M: Hartmann Number $[B_0 h(s/\mu)^{1/2}]$
p_s: Supply Pressure

Q: Flow rate
P_s^*: Dimensionless supply pressure
p: Lubricant pressure
P: Nondimensional pressure
w: Load carrying capacity
W: Dimensionless load carrying capacity
h_0': Surface width of lower plate
h_1': Surface width of upper plate
s_0: Electrical conductivity of lower surface
s_1: Electrical conductivity of upper surface
$\phi_0(h)$: Electrical permeability of lower surface ($s_0 h_0'/sh$)
$\phi_1(h)$: Electrical permeability of upper surface ($s_1 h_1'/sh$)
σ^*: Nondimensional standard deviation
α^*: Dimensionless variance
ε^*: Nondimensional skewness.

Data Availability

The data used to support the findings of this study are available from the corresponding author upon request.

Conflicts of Interest

The authors declare that they have no conflicts of interest.

References

[1] B. C. Majumdar, *Introduction to Tribology of Bearing*, Wheeler publishers, Wheeler Co .Ltd, 1985.

[2] J. Lin, "Static and dynamic characteristics of externally pressurized circular step thrust bearings lubricated with couple stress fluids," *Tribology International*, vol. 32, no. 4, pp. 207–216, 1999.

[3] G. M. Deheri, H. C. Patel, and R. M. Patel, "Performance of magnetic fluid based circular step bearings," *Mechanika*, vol. 57, no. 1, pp. 22–27, 2006.

[4] J. L. Neuringer and R. E. Rosensweig, "Magnetic fluids," *Physics of Fluids*, vol. 7, no. 12, pp. 1927–1937, 1964.

[5] H. Christensen and K. Tonder, "Tribology of rough surfaces: Parametric study and comparison of lubrication models," *SINTEF Report*, vol. 93, no. 3, pp. 324–329, 1969.

[6] H. Christensen and K. Tonder, "Tribology of rough surfaces: Stochastic models of hydrodynamic lubrications," *SINTEF Report*, vol. 93, no. 3, pp. 324–329, 1969.

[7] H. Christensen and K. Tonder, "Tribology of rough surfaces: A stochastic model of mixed lubrication," *SINTEF Report*, vol. 93, no. 3, pp. 324–329, 1970.

[8] L. L. Ting, "Engagement behavior of lubricated porous annular disks. Part I: squeeze film phase—surface roughness and elastic deformation effects," *Wear*, vol. 34, no. 2, pp. 159–172, 1975.

[9] J. Prakash and K. Tiwari, "Roughness effects in porous circular squeeze-plates with arbitrary wall thickness," *Journal of Lubrication Technology*, vol. 105, no. 1, pp. 90–95, 1983.

[10] B. L. Prajapati, *On Certain Theoretical Studies in Hydrodynamics And Elastohydrodynamics Lubrication [PhD. thesis]*, S. P. University, V. V. Nagar, India, 1995.

[11] P. I. Andharia, J. L. Gupta, and G. M. Deheri, "Effect of transverse surface roughness on the behavior of squeeze film in a spherical bearing," in *Proceedings of the International Conference: Problem of Non-Conventional Bearing Systems (NCBS '99)*, 1999.

[12] P. A. Vadher, P. C. Vinodkumar, G. M. Deheri, and R. M. Patel, "Behaviour of hydromagnetic squeeze films between two conducting rough porous circular plates," *Journal of Engineering Tribology*, vol. 222, no. 4, pp. 569–579, 2008.

[13] J. R. Patel and G. M. Deheri, "Shliomis model based magnetic fluid lubrication of a squeeze film in rotating rough curved circular plates, Cerib," *Journal of Science and Technology*, vol. 1, pp. 138–150, 2013.

[14] R. Patel, G. Deheri, and H. Patel, "Effect of transverse roughness on the performance of a circular step bearing lubricated with a magnetic fluid," *Annals*, vol. 8, no. 2, pp. 23–30, 2010.

[15] J.-R. Lin, L.-M. Chu, L.-J. Liang, and P.-H. Lee, "Derivation of a modified lubrication equation for hydromagnetic non-Newtonian cylindrical squeeze films and its application to circular plates," *Journal of Engineering Mathematics*, vol. 77, pp. 69–75, 2012.

[16] R. M. Patel and G. M. Deheri, "Magnetic fluid based squeeze film behavior between rotating porous circular plates with a concentric circular pocket and surface roughness effects," *International Journal of Applied Mechanics and Engineering*, vol. 8, no. 2, pp. 271–277, 2003.

[17] P. I. Andharia and G. M. Deheri, "Effect of longitudinal surface roughness on the behaviour of squeeze film in a spherical bearing," *International Journal of Applied Mechanics and Engineering*, vol. 6, no. 4, pp. 885–897, 2001.

[18] P. I. Andharia and G. Deheri, "Longitudinal roughness effect on magnetic fluid-based squeeze film between conical plates," *Industrial Lubrication and Tribology*, vol. 62, no. 5, pp. 285–291, 2010.

[19] P. I. Andharia and G. M. Deheri, "Performance of magnetic-fluid-based squeeze film between longitudinally rough elliptical plates," *ISRN Tribology*, vol. 2013, Article ID 482604, 6 pages, 2013.

[20] M. E. Shimpi and G. M. Deheri, "Combine effect of bearing deformation and longitudinal roughness on the performance of a ferrofluid based squeeze film together with velocity slip in truncated conical plates," *Imperial journal of Interdisciplinary research*, vol. 2, no. 8, pp. 1423–1430, 2016.

[21] J.-R. Lin, "Longitudinal surface roughness effects in magnetic fluid lubricated journal bearings," *Journal of Marine Science and Technology (Taiwan)*, vol. 24, no. 4, pp. 711–716, 2016.

[22] R. M. Patel, G. M. Deheri, and P. A. Vahder, "Hydromagnetic rough porous circular step bearing," *Eastern Academic Journal*, vol. 3, pp. 71–87, 2015.